Review

Mannose-binding analysis and biological application of pradimicins

By Yu NAKAGAWA[*1,*2,†] and Yukishige ITO[*2,*3,†]

(Edited by Keisuke SUZUKI, M.J.A.)

Abstract: Pradimicins (PRMs) are an exceptional family of natural products that specifically bind D-mannose (Man). In the past decade, their scientific significance has increased greatly, with the emergence of biological roles of Man-containing glycans. However, research into the use of PRMs has been severely limited by their inherent tendency to form water-insoluble aggregates. Recently, we have established a derivatization strategy to suppress PRM aggregation, providing an opportunity for practical application of PRMs in glycobiological research. This article first outlines the challenges in studying Man-binding mechanisms and structural modifications of PRMs, and then describes our approach to address them. We also present our recent attempts toward the development of PRM-based research tools.

Keywords: antibiotic, carbohydrate recognition, lectin mimic, molecular interaction, natural product, solid-state NMR

Introduction

There is a growing awareness that post-translational glycosylation plays more significant roles in protein functioning than previously estimated. Accumulated data suggest that a variety of proteins are glycosylated, and the glycan moieties not only affect the physicochemical properties of the proteins but also act as mediators in physiological events such as cell signaling, fertilization, embryogenesis, and neuronal development.[1),2)] There is also emerging evidence that glycans are closely involved in pathological events including innate immune response, inflammation, pathogen infection, and tumor progression.[3),4)] Thus, comprehensive studies of glycans are crucial to provide a proper understanding of biological processes.

Lectins, proteins of non-immune origin that bind a specific carbohydrate, have been employed to analyze the structure and function of glycans for decades, and these still provide great potential for future studies in glycobiology.[5)–7)] However, research use of lectins is sometimes limited by their cross reactivity, immunogenicity, and cytotoxicity. In addition, due to their proteinaceous nature, lectins are often expensive to manufacture, susceptible to enzymatic degradation, and unsuitable for long-term storage. These disadvantages of lectins lead to interest in non-peptidic small molecules that emulate the carbohydrate-binding properties of lectins.

It is generally quite challenging, however, to design small molecules that capture carbohydrates in aqueous media.[8)–10)] The essence of the problem lies in the competition between carbohydrates and water molecules (Fig. 1). As the arrangement of the hydroxy groups and endocyclic oxygen atom of carbohydrates is reproducible by water molecules, carbohydrates are seemingly indistinguishable from clusters of water molecules. Structural similarity among carbohydrates generates another problem of binding selectivity. For example, D-glucose (Glc) differs from D-mannose (Man), D-galactose (Gal), D-glucosamine, and *N*-acetyl-D-glucosamine (GlcNAc) only in one stereochemistry or in one functional group, and thus the complete discrimination of Glc

[*1] Institute for Glyco-core Research (iGCORE), Nagoya University, Nagoya, Aichi, Japan.
[*2] RIKEN Cluster for Pioneering Research, Wako, Saitama, Japan.
[*3] Graduate School of Science, Osaka University, Toyonaka, Osaka, Japan.
[†] Correspondence should be addressed: Y. Nakagawa, Institute for Glyco-core Research (iGCORE), Nagoya University, Furo-cho, Chikusa-ku, Nagoya, Aichi 464-8601, Japan (e-mail: yu@agr.nagoya-u.ac.jp); Y. Ito, Graduate School of Science, Osaka University, 1-1 Machikaneyama-cho, Toyonaka, Osaka 560-0043, Japan (e-mail: yukito1954@gmail.com).

doi: 10.2183/pjab.98.002

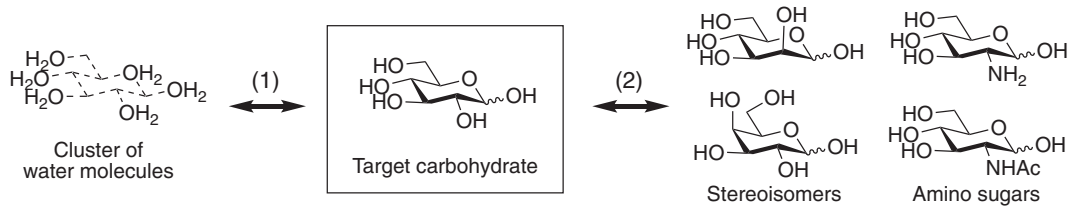

Fig. 1. Challenges for the development of carbohydrate-binding molecules. Carbohydrates are hard to distinguish from (1) clusters of water molecules and (2) stereoisomers and amino sugars.

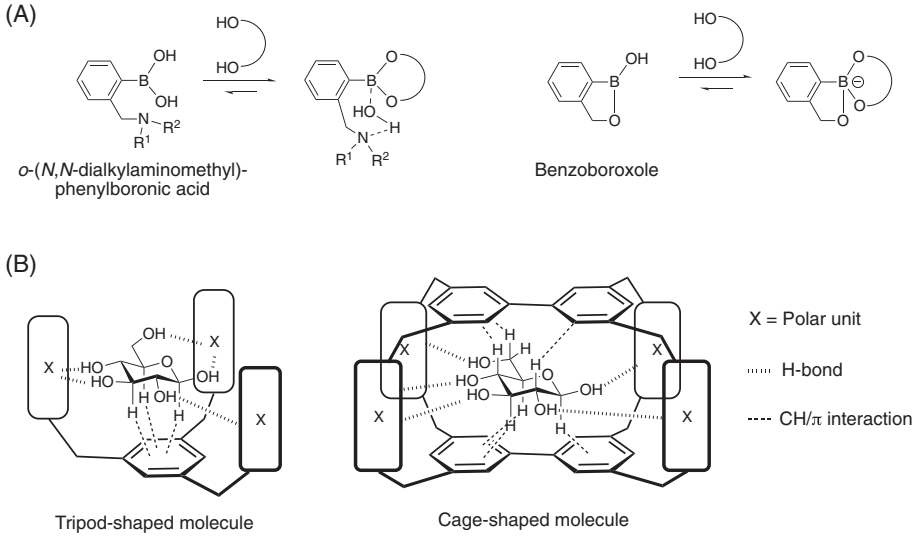

Fig. 2. Representative strategies for capturing carbohydrates. (A) *o*-(*N*,*N*-dialkylaminomethyl)phenylboronic acid and benzoboroxole form covalent bonds with 1,2- or 1,3-diol moieties of carbohydrates. (B) Tripod- and cage-shaped molecules accommodate carbohydrates through non-covalent bonds.

from other monosaccharides is a difficult task. Consequently, specific binding of the target carbohydrate in water is a major challenge in supramolecular chemistry.

In the last two decades, two major approaches have been intensively pursued to capture carbohydrates by non-protein structures (Fig. 2). One is the use of the reversible reaction between boronic acid and diols to give cyclic boronate esters.[11),12)] Although boronate esters are unstable at neutral pH, *o*-(*N*,*N*-dialkylaminomethyl)phenylboronic acid and benzoboroxole have been shown to form stable adducts with carbohydrates in physiologically relevant conditions. Another approach relies solely on non-covalent bonds for binding carbohydrates.[13),14)] Representative examples are tripod- and cage-shaped molecules, which accommodate carbohydrates through hydrogen bonding and CH/π interactions. The success in this area of research has significantly enhanced our understanding of factors contributing to the recognition of carbohydrates. However, there still remains a general lack of compounds that bind to biologically important glycans, and thus glycobiological application of synthetic molecules is still in the early stage of investigation.

On the other hand, nature has created a unique family of small molecules with lectin-like ability. Pradimicins (PRMs) and benanomicins (BNMs) are actinomycete-derived antibiotics that bind Man in aqueous media (Fig. 3).[15)–17)] They completely discriminate Man from the other common monosaccharides including Glc, Gal, GlcNAc, *N*-acetyl-D-galactosamine, and L-fucose (Fuc). Such binding specificity for Man has never been observed in existing synthetic molecules. In addition, PRMs and BNMs have the capacity to bind Man residues in glycans of biological and pathological importance,[18)–20)] highlighting their great potential for use as lectin mimics. However, despite the commercial availability of some members of the PRMs and

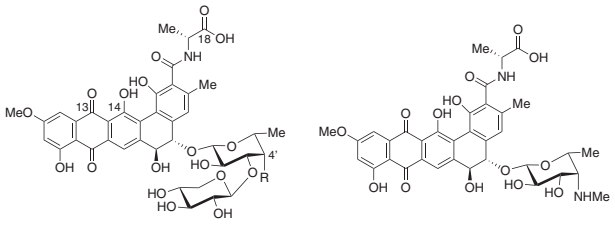

Fig. 3. Structures of pradimicins (PRMs) and benanomicins (BNMs). PRM-C and BNM-B are structurally the same, but were independently reported by Oki *et al.*[15] and Takeuchi *et al.*,[16] respectively.

BNMs, only limited efforts have been made to explore their glycobiological applications. In this review, we first outline early studies on PRMs and BNMs, focusing on the reasons underlying their limited research use. We then summarize our studies on Man recognition by PRMs and also describe our recent attempts toward the development of PRM-based research tools.

1. Early studies on PRMs and BNMs

In 1988, the first members of the PRMs (PRM-A, B, C) and BNMs (BNM-A, B) were reported by Oki *et al.*[15] and Takeuchi *et al.*,[16] respectively (Fig. 3). Since then, more than ten members of the PRMs have been isolated and characterized.[17),21)–24)] These compounds have a common benzo[*a*]naphthacenequinone skeleton and inhibit the growth of a broad range of fungi with no cross-resistance to major antifungal agents, such as amphotericin B, 5-fluorocytosine, and ketoconazole.[17)] Subsequent studies on their mode of action revealed that the antifungal activity of PRMs and BNMs is closely related to their binding to cell wall mannans of fungi,[25),26)] which led to the finding that this family of antibiotics has a lectin-like ability to bind Man in a Ca^{2+}-dependent manner.[27)]

In the early 1990's, the Man binding mechanism of PRMs was studied intensively. Initial analysis found that PRMs co-precipitate with Man in the presence of Ca^{2+} to form water-insoluble aggregates, mainly consisting of a [$PRM_2/Ca^{2+}/Man_4$] complex.[27)–29)] Subsequent spectrophotometric studies suggested a step-wise formation of the complex (Fig. 4A): 1) two molecules of PRMs initially form the dimeric [PRM_2/Ca^{2+}] complex, 2) the PRM dimer binds two molecules of Man with high affinity, 3) the resulting [$PRM_2/Ca^{2+}/Man_2$] complex further accommodates two molecules of Man with low affinity to afford the ultimate [$PRM_2/Ca^{2+}/Man_4$] complex.[30)]

Although the complex-forming process of PRMs with Man was largely understood in the late 1990's, until recently the complex structures had not been elucidated. There are several reasons for the stagnation of the structural analysis. First, PRMs have a high propensity to aggregate in the presence of Ca^{2+}, making it difficult to analyze the complex structures using X-ray crystallographic and solution NMR spectroscopic approaches. Second, in dilute conditions that minimize aggregation, the [PRM_2/Ca^{2+}], [$PRM_2/Ca^{2+}/Man_2$], [$PRM_2/Ca^{2+}/Man_4$] complexes and their mixed oligomers co-exist in solution. This complicated equilibrium is also a major obstacle to solution NMR analysis. Third, NMR signals of the disaccharide moiety of PRMs overlap with those of Man. Isotopic labeling of PRMs is mandatory to overcome this problem, but chemical synthesis of PRMs requires a large number of steps,[31)] and thus is unlikely to be applicable to the efficient preparation of labeled PRMs. These issues have collectively frustrated further studies on the Man binding mechanism of PRMs.

In this situation, the hypothetical structure of the [PRM_2/Ca^{2+}] complex was proposed in 1993 (Fig. 4B).[28)] Based on the observation that methyl or ethyl ester derivatives of PRMs formed no Ca^{2+} complex, Ca^{2+} was assumed to bridge the C18 carboxyl groups of two PRM molecules in the [PRM_2/Ca^{2+}] complex. This Ca^{2+} binding model further led to the assumption that the C18 carboxyl group of PRMs cannot be altered for derivatization. Consequently, the C4′ amino group on the D-thomosamine moiety has been identified as the only conceivable site of facial modification toward glycobiological application of PRMs.[32)] However, the reactivity of the amino group is low, and effective derivatization at this position is still to be established. A recent example is Enomoto's work regarding the preparation of PRM-functionalized gold nanoparticles, in which the reaction of PRMs with a 2-bromoacetamide derivative gave a yield of 4′-*N*-carboxymethyated PRMs of only in 9%.[33)] These circumstances have severely limited the glycobiological application of PRMs.

2. Identification of the primary Man binding site of PRMs

In order to circumvent the above issues related to the analysis of the complex structures, we explored a conceptually novel analytical strategy using solid-

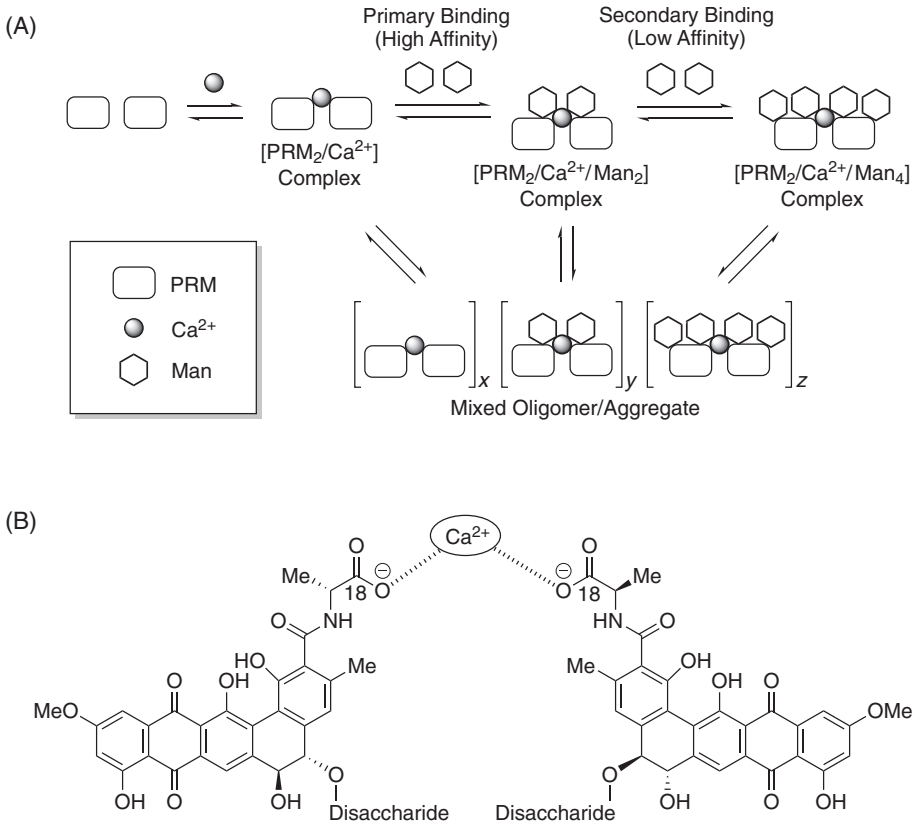

Fig. 4. (A) Complex formation of PRMs with Ca^{2+} and Man. PRMs initially form a [PRM_2/Ca^{2+}] complex, which then binds two molecules of Man with high affinity (primary binding). The resulting [$PRM_2/Ca^{2+}/Man_2$] complex accommodates another two molecules of Man with low affinity (secondary binding) to give the [$PRM_2/Ca^{2+}/Man_4$] complex. These three complexes randomly assemble to form the mixed oligomers or aggregates. (B) Putative structure of the [PRM_2/Ca^{2+}] complex.[28] Two molecules of PRMs are bridged by Ca^{2+} through their C18 carboxylate groups.

state NMR spectroscopy. In contrast to previous efforts that have failed to avoid the aggregation of PRMs, our approach actually makes use of the high aggregation properties of PRM-A, an original member of the PRMs (Fig. 3).[15] The strategy was based on the finding that when an aggregate consisting of the [PRM-$A_2/Ca^{2+}/Man_4$] complex was washed with an aqueous $CaCl_2$ solution, Man was selectively removed from the secondary binding sites to produce an aggregate mainly composed of the [PRM-$A_2/Ca^{2+}/Man_2$] complex (Fig. 5A).[34),35] The use of this solid aggregate eliminated the issue regarding the complicated equilibrium in solution, while enabling one-to-one interaction analysis of PRM-A and Man using solid-state NMR spectroscopy.

As a preliminary experiment, we performed solid-state cross polarization-magic angle spinning (CP-MAS) ^{13}C-NMR using a solid sample of the [PRM-$A_2/Ca^{2+}/Man_2$] complex. The ^{13}C signals of the [PRM-$A_2/Ca^{2+}/Man_2$] complex were significantly sharper and more distinguishable than those of freeze-dried PRM-A (Fig. 5B), indicating the higher structural homogeneity of the complex.[36] This encouraging result inspired us to exploit a two-dimensional dipolar-assisted rotational resonance (2D-DARR) methodology[37),38] for investigating Man binding geometry in the [PRM-$A_2/Ca^{2+}/Man_2$] complex. DARR, also known as RF-assisted diffusion (RAD),[39] is a technique in solid-state NMR spectroscopy to detect weak ^{13}C–^{13}C couplings in the presence of strong couplings derived from directly bound carbons. In 2D-DARR spectra, multiple ^{13}C–^{13}C restrains (~6 Å) can be simultaneously obtained from cross-peak intensities, allowing us to evaluate interatomic close contacts between PRM-A and Man in the [PRM-$A_2/Ca^{2+}/Man_2$] complex.

The remaining issue to be addressed is the isotopic labeling of PRM-A. In the case of the DARR

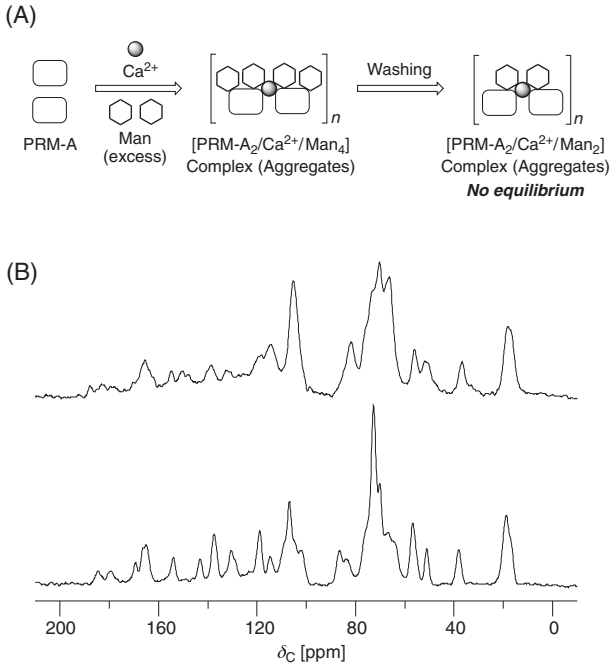

Fig. 5. (A) Sample preparation for solid-state NMR analysis. When PRM-A is mixed with excess amounts of Ca^{2+} and Man, an aggregate of the [$PRM_2/Ca^{2+}/Man_4$] complex precipitated. Extensive washing of the aggregate resulted in a release of Man from the secondary binding sites to produce the solid sample of the [$PRM_2/Ca^{2+}/Man_2$] complex. (B) Solid-state CP/MAS ^{13}C-NMR spectra of freeze-dried PRM-A (upper) and the aggregates of the [$PRM\text{-}A_2/Ca^{2+}/Man_2$] complex (lower).

experiments, selective ^{13}C-enrichment was necessary for enhancing the spectral sensitivity and for facilitating data interpretation. Considering the difficulties of the chemical synthesis of PRMs, we focused on the biosynthesis of PRM-A (Fig. 6A). Earlier studies showed that D-alanine was directly incorporated into the D-alanine moiety of PRM-A, and 11-*O*- and 4′-*N*-methyl groups were derived from *S*-adenosylmethinonine.[40),41)] Based on this biosynthetic pathway, we conducted feeding experiments using *Actinomadura* sp. TP-A0019, a PRM-A-producing actinomycete. As expected, feeding of D-[$^{13}C_3$]alanine and L-[5-$^{13}CH_3$]methionine successfully provided PRM-A with an ^{13}C-enriched D-alanine moiety (*ca.* 70 atom % ^{13}C) and two methyl groups (*ca.* 65 atom % ^{13}C), respectively (Fig. 6B).[35)]

Using the ^{13}C-enriched PRM-As ([$^{13}C_3$]- and [$^{13}C_2$]PRM-As) and readily available methyl α-D-[$^{13}C_6$]mannopyranoside ([$^{13}C_6$]Man-OMe), we prepared their [$PRM_2/Ca^{2+}/Man_2$] complexes as solid aggregates. Figure 7 shows 2D-DARR spectra of these samples.[35)] In the spectrum of the complex of [$^{13}C_3$]PRM-A (Fig. 7A), mixing time-dependent cross peaks were clearly observed between ^{13}C signals for the D-alanine moiety of [$^{13}C_3$]PRM-A ($\delta = 20.0$ ppm for 17-Me, $\delta = 50.8$ ppm for C17, $\delta = 179.8$ ppm for C18) and those for [$^{13}C_6$]Man-OMe ($\delta = 63.0$, 68.2, 71–76 ppm for C2–C6, $\delta = 101.4$ ppm for C1), indicating the close contact of Man-OMe with the D-alanine moiety of PRM-A. On the other hand, intermolecular cross peaks were hardly observed in the spectra of the complex of [$^{13}C_2$]PRM-A (Fig. 7B). This observation eliminates the possibility that the cross peaks observed in the spectrum of [$^{13}C_3$]PRM-A were derived from accidental proximity in the solid sample, and also suggested that 11-*O*-methyl and 4′-*N*-methyl groups of PRM-A are relatively far from Man-OMe in the complex. These combined results indicated that Man is located within 6 Å of the D-alanine moiety of PRM-A in the [$PRM_2/Ca^{2+}/Man_2$] complex.

Following the suggestion that the D-alanine moiety may be a part of the primary Man binding site of PRM-A, we then explored the Man binding geometry. Additional feeding experiments found that DL-[$^{13}C_3$]alanine feeding increased the ^{13}C-population of the benzo[*a*]naphthacenequinone moiety (*ca.* 15 atom % ^{13}C) of PRM-A as well as the D-alanine moiety (Fig. 6).[42)] This was probably due to the metabolic conversion of L-[$^{13}C_3$]alanine to [$^{13}C_2$]acetyl-CoA, which comprised the aromatic region of PRM-A *via* a polyketide pathway.[40)] Although ^{13}C enrichment of the aromatic ring was low, the resulting [$^{13}C_{27}$]PRM-A was expected to provide comprehensive information regarding interatomic distances between PRM-A and Man in the [$PRM_2/Ca^{2+}/Man_2$] complex. Thus, we performed systematic 2D-DARR experiments using [$^{13}C_{27}$]PRM-A and singly ^{13}C-labeled Man-OMe.[42)]

The DARR spectra (Fig. 7C) showed that the complexes of [$^{13}C_{27}$]PRM-A with [2-^{13}C]-, [3-^{13}C]-, and [4-^{13}C]Man-OMe gave significant cross peaks between the ^{13}C signals for the labeled positions of Man-OMe and those for the D-alanine moiety (C17, 17-Me, C18) of PRM-A. In contrast, only faint or negligible intermolecular cross peaks were observed in the complexes with [1-^{13}C]-, [5-^{13}C]-, and [6-^{13}C]Man-OMe, indicating that the C2–C4 positions of Man were proximal to the D-alanine moiety of PRM-A in the [$PRM_2/Ca^{2+}/Man_2$] complex. Regarding the aromatic ring of PRM-A, weak cross peaks with the C14 and C15 signals of PRM-A were detected in the complex with [2-^{13}C]Man-OMe. The C3 signal of [3-^{13}C]Man-OMe also gave a weak cross-

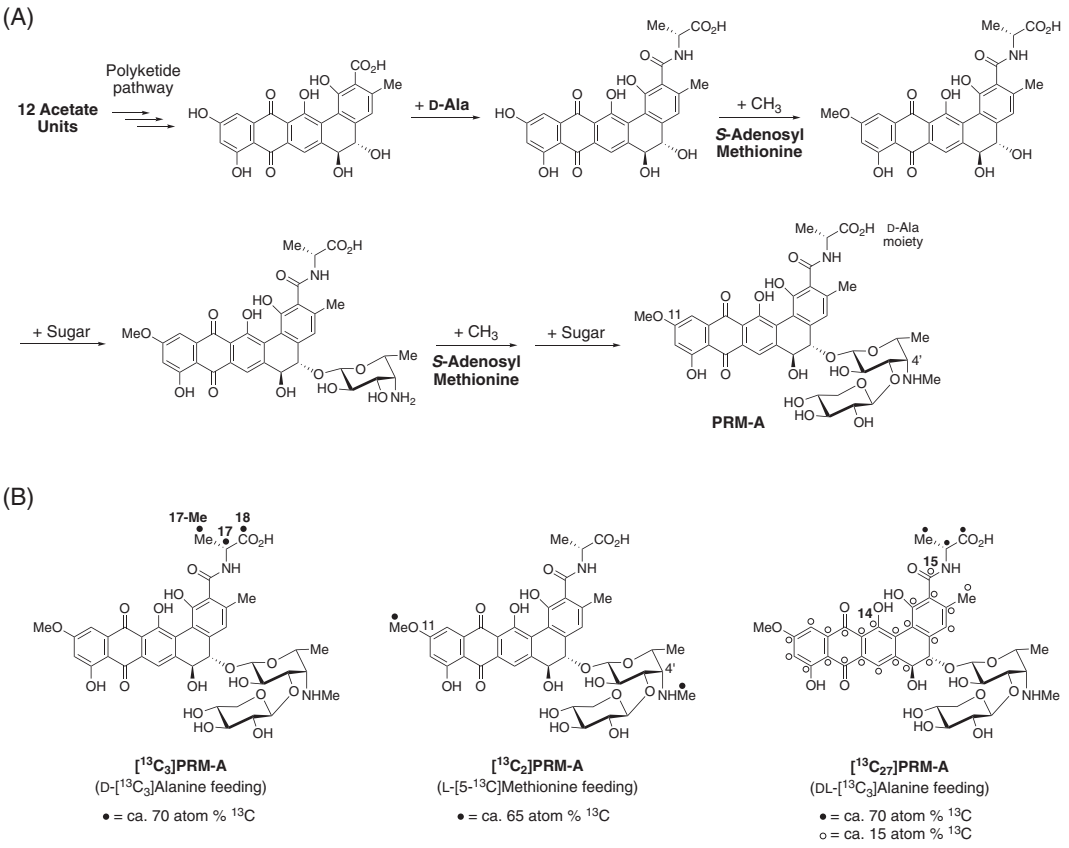

Fig. 6. (A) Outline of biosynthetic pathway for PRM-A. (B) Biosynthetically ^{13}C-enriched PRM-As. Black and open circles indicate ^{13}C-enriched positions. Whereas D-[$^{13}C_3$]alanine was exclusively introduced to the D-alanine moiety of PRM-A, DL-[$^{13}C_3$]alanine feeding increased the ^{13}C-population of D-alanine moiety and the aromatic region probably through the metabolic conversion of L-[$^{13}C_3$]alanine to [$^{13}C_2$]acetyl-CoA. Feeding of ^{13}C-labeled NaOAc similarly increased the ^{13}C-population of the aromatic region, but severely inhibited the growth of the actinomycete, resulting in the low isolation yield of ^{13}C-labeled PRM-A. The ^{13}C population was calculated from the solution ^{1}H-NMR data on the basis of integration values of proton signals split with ^{1}H–^{13}C couplings.

peak with the C14 signal of [$^{13}C_{27}$]PRM-A. Although full detection of close contacts between the aromatic region of PRM-A and Man was not achieved due to the low ^{13}C-enrichment, it was quite likely that the C2 and C3 positions of Man were in close contact with the aromatic region of PRM-A. These results collectively suggested the Man binding geometry of PRM-A, in which the C2–4 region of Man was located close to D-alanine moiety of PRM-A, with the C2 position oriented toward the benzo[*a*]naphthacenequinone moiety (Fig. 7D).

3. Estimation of the [PRM$_2$/Ca^{2+}/Man$_2$] complex

Although distance information between PRM-A and Man in the [PRM-A$_2$/Ca^{2+}/Man$_2$] complex has been accumulated, a lack of data regarding the geometry of Ca^{2+} coordination prevented us from estimating the mode of Man binding. Our initial attempt to explore this issue was made by solid-state ^{113}Cd-NMR investigation using $^{113}Cd^{2+}$ with a spin of 1/2 as a surrogate probe for Ca^{2+} with a spin of 7/2.[34] Based on the previous report that PRMs bound Man in the presence of Cd^{2+},[27] the [PRM-A$_2$/$^{113}Cd^{2+}$] complex was prepared as aggregates, and subjected to solid-state ^{113}Cd-NMR analysis. Although the chemical shift of the ^{113}Cd signal in the 1D spectrum of the complex gave no information regarding the geometric arrangement of $^{113}Cd^{2+}$ coordination, subsequent rotational-echo double resonance (REDOR) and ^{111}Cd frequency-selective REDOR (FSR) experiments using the $^{111}Cd^{2+}$ probe gave an unexpected result.[43] Evaluation of ^{13}C–^{111}Cd distances in the [PRM-A$_2$/$^{111}Cd^{2+}$] complex revealed that $^{111}Cd^{2+}$ is located near the C13 and C14 positions of PRM-A, but relatively far from the

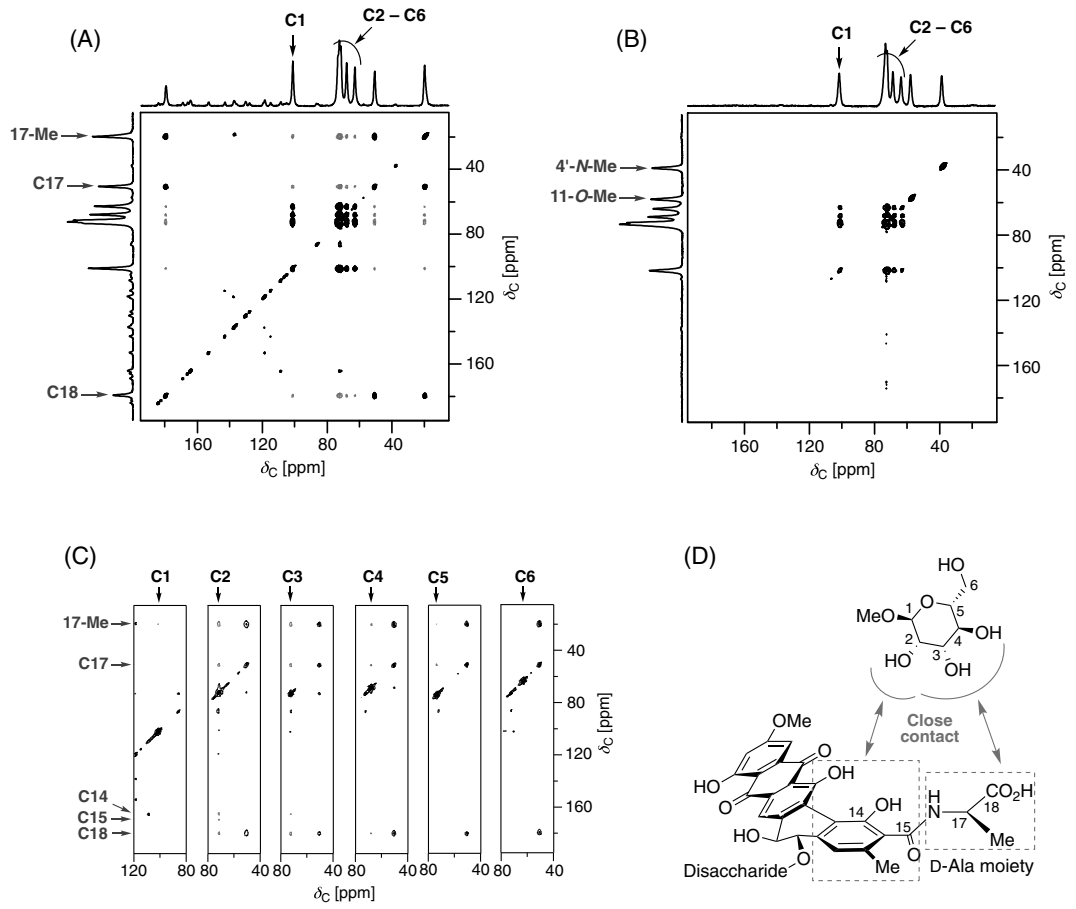

Fig. 7. (Color online) 2D-DARR spectra of the [$PRM_2/Ca^{2+}/Man_2$] complexes of (A) [$^{13}C_3$]PRM-A and [$^{13}C_6$]Man-OMe and (B) [$^{13}C_2$]PRM-A and [$^{13}C_6$]Man-OMe. Blue and black arrows represent ^{13}C signals for ^{13}C-enriched PRM-A and [$^{13}C_6$]Man-OMe, respectively. Mixing time-dependent intermolecular cross peaks are shown in red. (C) 2D-DARR spectra of the [$PRM_2/Ca^{2+}/Man_2$] complexes of [$^{13}C_{27}$]PRM-A and singly ^{13}C-labeled Man-OMe. Blue and black arrows represent ^{13}C signals for ^{13}C-enriched PRM-A and singly ^{13}C-labeled Man-OMe, respectively. Mixing time-dependent intermolecular cross peaks are shown in red. (D) Relative geometry of PRM-A and Man-OMe in the complex from DARR analysis.

C18 position. This suggests that Ca^{2+} is coordinated with the C13 carbonyl and C14 hydroxyl groups of PRM, which was contradictory to the previous assumption that the C18 carboxyl group is the Ca^{2+} binding site of PRM-A.[28)]

The implication for our solid-state NMR analysis was confirmed using the crystal structure of the [PRM_2/Ca^{2+}] complex.[44)] We successfully prepared X-ray quality crystals of the Ca^{2+} complex using BMY-28864 (**1**), a D-serine analog of PRM-A with improved water solubility (Fig. 8A).[45)] X-ray crystallographic analysis revealed that the C13 carbonyl and C14 hydroxyl groups of **1** coordinated with Ca^{2+} to bridge the benzo[*a*]naphthacenequinone moieties of two molecules of **1** (Fig. 8B). In this face-to-face geometry, the hydrophilic moieties (Ca^{2+}, D-serine, and disaccharide moieties) were arranged around the hydrophobic aromatic rings. Given that this arrangement was favored in aqueous media, esterification of the C18 carboxyl group of PRM-A may destabilize the dimeric structure due to the decreasing hydrophilicity at the D-alanine moiety, which likely explained why methyl and ethyl esters of PRM-A lack the ability to form the Ca^{2+} complex.

Based on this dimeric structure and accumulated information on the Man binding geometry of PRM-A, we estimated a structure of the [PRM-A_2/Ca^{2+}/Man-OMe_2] complex through density functional theory calculations at the ωB97X-D/6-31G(d) level (Fig. 8C).[44)] In the energy-minimized structure, two molecules of Man-OMe bound to the [PRM-A_2/Ca^{2+}] complex in a symmetrical manner.

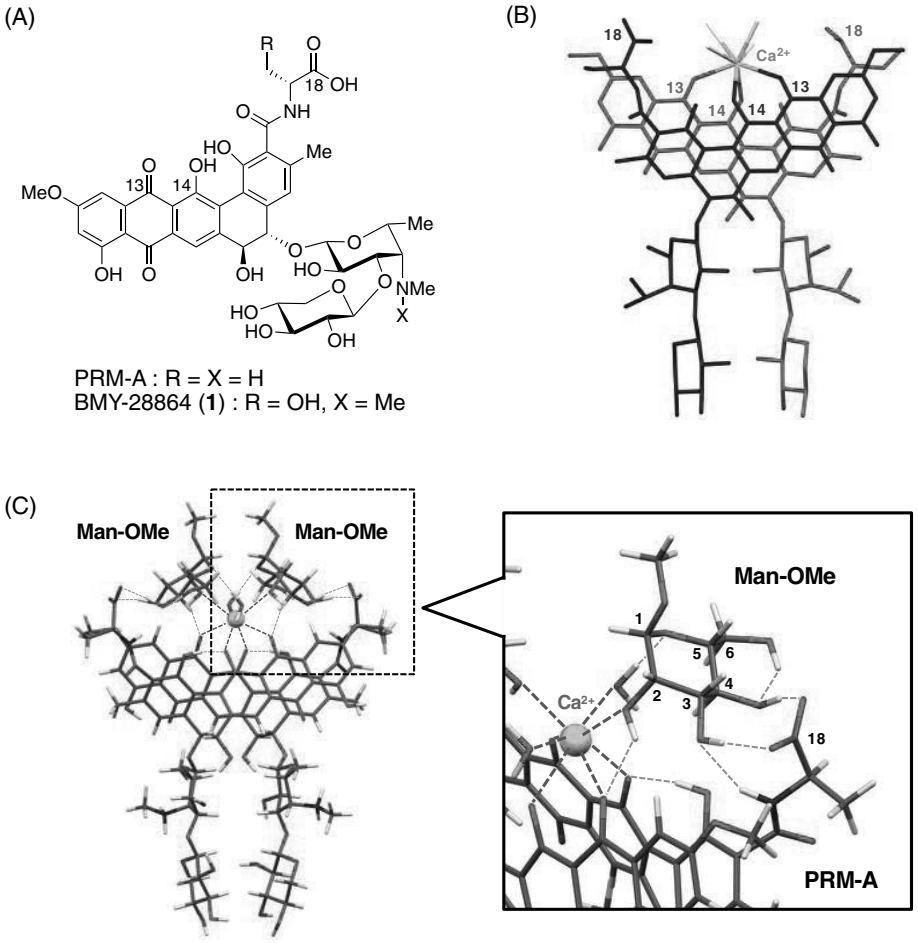

Fig. 8. (Color online) (A) Structures of PRM-A and BMY-28864 (**1**). (B) Crystal structure of the [$\mathbf{1}_2$/Ca^{2+}] complex. Two molecules of **1** are separately shown in red and blue. Hydrogen atoms are omitted for clarity. (C) Energy-minimized structure of the [PRM-A_2/Ca^{2+}/Man-OMe_2] complex obtained using solid-state NMR-based density functional theory calculations. Carbon, oxygen, nitrogen, hydrogen, and calcium atoms are shown in gray, red, blue, white, and green, respectively. Hydrogen bonding and Ca^{2+} coordination are indicated as blue and green dotted lines, respectively.

The 2-, 3-, and 4-hydroxyl groups of Man-OMe were involved in Ca^{2+}-coordination and/or hydrogen bonds with PRM-A, whereas the 1-methoxy and 6-hydroxyl groups did not interact with either Ca^{2+} or PRM-A. The endocyclic oxygen atom in the pyranose ring of Man-OMe also contributed to the complex formation as an acceptor for hydrogen bonding with the Ca^{2+}-coordinated water molecule. This mode of Man recognition was in good agreement with the fact that PRM-A formed a complex with 6-deoxy-Man-OMe but not with 2-, 3-, and 4-deoxy-Man-OMe.[42] The contribution of the endocyclic oxygen atom of Man-OMe was also supported by the demonstration that replacement of the oxygen atom of Man-OMe with the less polar sulfur atom resulted in a significant decrease in binding affinity for PRMs.[46]

4. Binding evaluation of PRMs for oligomannoses

Following elucidation of the molecular basis of Man recognition by PRMs, our attention was turned to oligomannose binding of PRMs. There have been several early studies suggesting that PRMs might prefer oligomannoses over Man. For example, UV-visible spectrophotometric analysis by Fujikawa *et al.*[30] and NMR spectroscopic analysis by Shahzad-ul-Hussan *et al.*[47] both demonstrated that PRMs showed much higher affinity for 3,6-di-*O*-α-D-mannopyranosyl-α-D-mannopyranose than Man. However, further binding studies using structurally well-defined oligomannoses have yet to be carried out, leaving the binding preference of PRMs for other

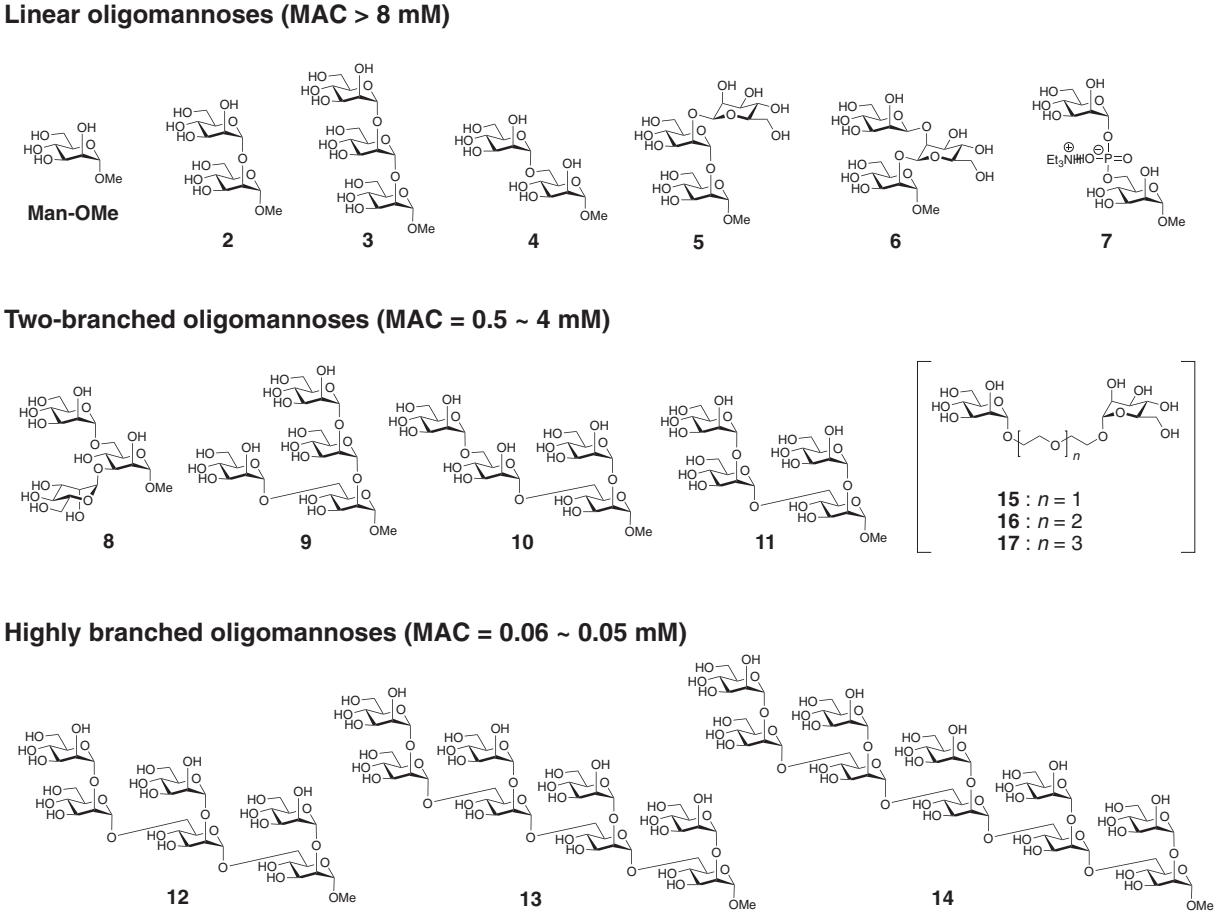

Fig. 9. Structures of synthetic oligomannoses (**2**–**14**) and oligomannose mimics (**15**–**17**). The approximate values of their MACs are also shown. MAC: minimum antagonistic concentration required to suppress PRM-A (32 μg/mL)-induced growth inhibition of *C. rugosa* cells.

oligomannoses unclear. Thus, we evaluated the binding affinity of PRMs with thirteen oligomannoses (**2**–**14**; Fig. 9),[48] which reflected the structural motifs characteristic of the cell wall mannans from *Candida albicans*.[49]

Oligomannoses (**2**–**14**) were synthesized via a stepwise or blockwise glycosylation strategy using thiomannoside[50] and mannosyl halide donors.[51),52] To estimate the relative binding affinity of PRM-A for these oligomannoses, we examined their antagonistic effects on the antifungal activity of PRM-A against *Candida rugosa*. Comparison of their minimum antagonistic concentrations (MACs) required for suppressing PRM-A (32 μg/mL)-induced growth inhibition of *C. rugosa* cells revealed that branched oligomannoses (**8**–**14**) with multiple non-reducing ends suppressed the antifungal activity of PRM-A more potently than Man-OMe and the linear oligomannoses (**2**–**7**), and the antagonistic effect of the branched oligomannoses correlated with the number of Man residues at their non-reducing ends. In addition, oligomannose mimics (**15**–**17**), in which two mannose units were connected by polyethylene glycol spacers, were found to exhibit MACs similar to those of two-branched oligomannoses (**8**–**11**). These results collectively indicated that PRMs bind to the Man residues at the non-reducing ends of oligomannoses, and the binding affinity was highly dependent on the number of terminal Man residues of oligomannoses.

5. Application of PRMs for glycobiological research

Upon receiving confirmation that Man recognition is the key to oligomannose binding of PRMs, we then wished to derivatize PRM-A for research use based on our Man binding model (Fig. 8C). As our crystallographic analysis has disproved the previous

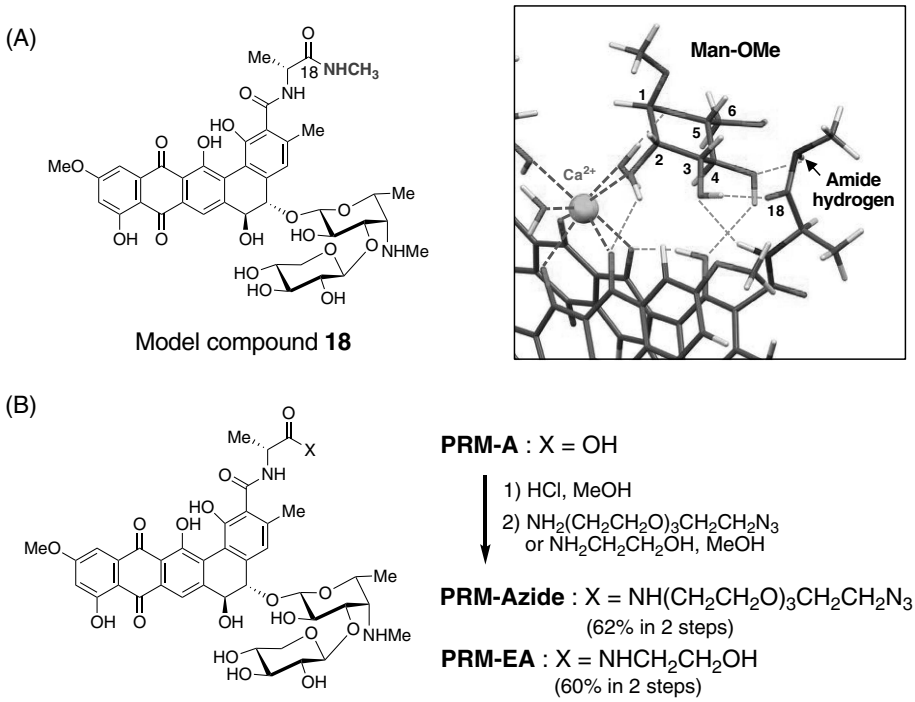

Fig. 10. (Color online) (A) Structure of model compound **18** (left) and possible interaction of **18** with Man-OMe estimated through preliminary molecular modeling (right). Carbon, oxygen, nitrogen, hydrogen, and calcium atoms are shown in gray, red, blue, white, and green, respectively. Hydrogen bonding and Ca^{2+} coordination are indicated as blue and green dotted lines, respectively. (B) Two-step preparation of PRM-Azide and PRM-EA.

assumption that the carboxylate form of PRMs is required for the formation of the Ca^{2+} complex (Fig. 4B), we explored modification at the C18 carboxyl group of PRM-A. The *in silico* study using model compound **18** (Fig. 10A) suggested that introduction of *N*-methylamide at the C18 carboxylate of PRM-A could maintain the interaction with the 2-, 3-, and 4-hydroxyl groups of Man, with the amide hydrogen acting as a hydrogen-bond donor to the 4-hydroxyl group of Man.[44] It was also proposed that the methyl group on the amide nitrogen of **18** would face outward from the binding site, and thus functional units can be attached *via* the amide linkage without interfering with the hydrogen bond network. From a synthetic viewpoint, amide formation would be easily performed through an ester/amide exchange reaction using PRM-A methyl ester[53] without protection of other functional groups within the molecule.

Based on these considerations, we designed PRM-Azide, in which 11-azido-3,6,9-trioxaundecan-1-amine was introduced onto the C18 carboxyl group of PRM-A through an amide linkage (Fig. 10B).[44] PRM-Azide was readily synthesized from PRM-A in two steps (62%), consisting of methyl esterification and ester/amide exchange reaction. Binding tests by isothermal titration calorimetry (ITC) revealed that this derivatization did not have a major deleterious effect on the binding affinity for Man-OMe ($K_d =$ 513 μM for PRM-Azide, $K_d = 96$ μM for PRM-A). A control experiment in the absence of Ca^{2+} hardly detected any heat change, supporting that PRM-Azide requires the formation of the Ca^{2+} complex for Man binding like PRM-A. Of further significance, PRM-Azide was found to be insensitive to other common monosaccharides including Glc, Gal, GlcNAc, NeuNAc, and Fuc, suggesting its high binding selectivity for Man. These encouraging results prompted us to explore the application of PRM-Azide to fluorescent staining of cell-wall mannans using living fungal cells. Among the various protocols tested, clear fluorescence was observed on the cell surface of *C. rugosa* (Fig. 11) when the fungal cells were treated with PRM-Azide followed by attachment of a fluorescent tag through a copper-catalyzed azide-alkyne cycloaddition (CuACC) reaction with the TAMRA-alkyne.[44] The staining was markedly suppressed in the presence of exogenous mannans derived from *Saccharomyces cerevisiae*, and only faint fluorescence was detected in the same

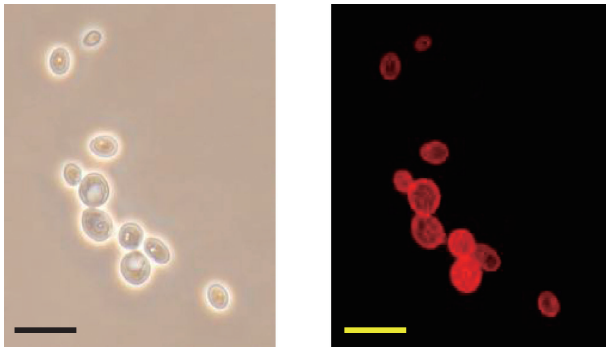

Fig. 11. Fluorescent staining of *C. rugosa* (left: phase-contrast image, right: fluorescent image, scale bars: 10 µm). Treatment of the fungal cells with PRM-Azide in the presence of $CaCl_2$ followed by conjugation of the TAMRA-alkyne fluorescently stains the cell-wall mannans.

experiment using *Escherichia coli*, which contained GlcNAc and *N*-acetylmuramic acid (MurNAc) in their cell-wall glycans. These combined results clearly indicated that the observed fluorescence arose from the binding of PRM-Azide to cell-wall mannans of *C. rugosa*, thereby highlighting the potential of PRM-Azide as a research tool for fluorescent staining of Man-containing glycans.

During the staining experiments with *C. rugosa*, we observed that PRM-Azide aggregated less than PRM-A. This observation was further supported using a sedimentation assay, which demonstrated that, although PRM-A completely aggregated in Ca^{2+}-containing neutral buffer, more than 95% of PRM-Azide was detected in the supernatant. This finding raised the possibility that the aggregation of PRM-A may be suppressed by the installation of hydrophilic moieties into its C18 carboxyl group *via* the amide linkage. Thus, we synthesized a simpler amide derivative, PRM-EA, in which hydrophilic 2-aminoethanol was attached to the C18 carboxyl group of PRM-A (Fig. 10B).[54] As we expected, PRM-EA was found to be markedly less aggregative than PRM-A, while retaining Ca^{2+}-dependent Man binding. These favorable properties of PRM-EA along with its inherent red color allowed us to utilize on-membrane detection of glycoproteins. Dot blot assays demonstrated that PRM-EA was able to stain ovalbumin (OVA)[55] and thyroglobulin (Tg)[56] carrying high mannose-type and hybrid-type N-linked glycans with terminal Man residues, but not fetuin (Fet),[57] transferrin (TRF),[58] or immunoglobulin G (IgG)[59] carrying complex-type N-linked glycans with terminal Gal or NeuNAc residues (Fig. 12). Such staining selectivity has never been observed in

Protein	Main glycan type
Thyroglobulin (Tg)	High mannose, Hybrid
Ovalbumin (OVA)	High mannose, Complex
Fetuin (Fet)	Complex
Transferrin (TRF)	Complex
Immunoglobulin G (IgG)	Complex

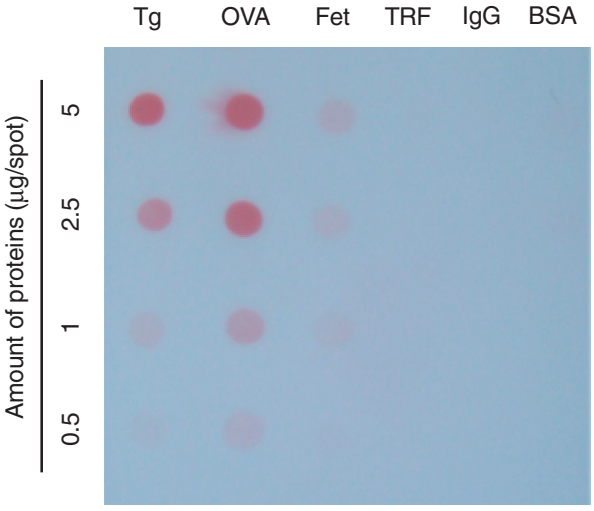

Fig. 12. Dot blot assay for glycoproteins (Tg, OVA, Fet, TRF, IgG) using PRM-EA as a staining agent. BSA without glycans was also spotted as a negative control (right end line).

conventional dyes, suggesting that PRM-EA may serve as a unique dye for the selective detection of terminal Man-containing glycoproteins.

6. Conclusion and future prospects

Despite growing interest in the biological roles of Man-containing glycans, there has been a paucity of small molecule-derived tools to investigate glycan functions. PRMs and BNMs constitute a unique family of natural products capable of binding to Man-containing glycans, and therein holding great promise as research tools in glycobiology. However, in spite of their commercial availability, practical applications have yet to be achieved due to severe aggregation in physiologically relevant conditions. Our mechanistic studies on the Man recognition by PRMs identified the C18 carboxyl group of PRM-A as a modifiable site, which led to the finding that attachment of hydrophilic units to the C18 carboxyl group significantly suppressed aggregation without impairing Man-binding specificity. The demonstration that PRM-Azide and PRM-EA can stain fungal cells and glycoproteins suggested that the amide

formation of PRMs may be a promising strategy for the design of PRM-based research tools.

Because the amide group acts as a linker to connect functional molecules, it is expected that various research tools can be developed by amide formation on PRMs. For example, PRM-conjugated agarose beads may be potentially used for the purification of Man-containing glycans or glycoproteins. Similarly, PRM-attached magnetic beads are likely to be applicable for the enrichment of Man-rich exosomes or viral particles. When considering the possible advantage of PRMs over protein lectins with regard to their high stability in a cellular environment and the ease of cellular uptake, amide derivatives with radiolabeled tags have the potential to be used for positron emission tomography imaging of intracellular glycans. The studies described herein offer a unique opportunity for exploring practical applications of PRMs in glycobiological research.

Acknowledgement

This research was conducted in collaboration with Dr. Daisuke Hashizume of RIKEN, Prof. Yasuhiro Igarashi of Toyama Prefectural University, Prof. Kiyonori Takegoshi and Dr. Takashi Doi of Kyoto University, Prof. Misako Aida and Dr. Dai Akase of Hiroshima University, and Prof. Makoto Ojika of Nagoya University. The work was partly supported by a Grants-in-Aid for JSPS KAKENHI Grant (No. 22780109, 24102535, 15H04496, 19K05712) and SUNBOR grant from the Suntory Foundation of Life Sciences.

References

1) Paulson, J.C., Blixt, O. and Collins, B.E. (2006) Sweet spots in functional glycomics. Nat. Chem. Biol. **2**, 238–248.
2) Varki, A. (2017) Biological roles of glycans. Glycobiology **27**, 3–49.
3) Ohtsubo, K. and Marth, J.D. (2006) Glycosylation in cellular mechanisms of health and disease. Cell **126**, 855–867.
4) Pinho, S.S. and Reis, C.A. (2015) Glycosylation in cancer: Mechanisms and clinical implications. Nat. Rev. Cancer **15**, 540–555.
5) Alley, W.R., Jr., Mann, B.F. and Novotny, M.V. (2013) High-sensitivity analytical approaches for the structural characterization of glycoproteins. Chem. Rev. **113**, 2668–2732.
6) Dan, X., Liu, W. and Ng, T.B. (2016) Development and applications of lectins as biological tools in biomedical research. Med. Res. Rev. **36**, 221–247.
7) Hendrickson, O.D. and Zherdev, A.V. (2018) Analytical application of lectins. Crit. Rev. Anal. Chem. **48**, 279–292.
8) Davis, A.P. (2009) Synthetic lectins. Org. Biomol. Chem. **7**, 3629–3638.
9) Yang, X., Cheng, Y. and Wang, B. (2011). Synthetic lectin mimics artificial carbohydrate receptors. *In* Carbohydrate Recognition: Biological Problems, Methods, and Applications (eds. Wang, B. and Boons, G.-J.). Wiley, Hoboken, pp. 301–327.
10) Draganov, A., Wang, D., Holmes, J., Ji, K., Wang, B., Shaw, S.K. *et al.* (2015) Synthetic receptors for carbohydrates. *In* Synthetic Receptors for Biomolecules (ed. Smith, B.D.). The Royal Society of Chemistry, Cambridge, pp. 177–203.
11) Sun, X., Chapin, B.M., Metola, P., Collins, B., Wang, B., James, T.D. *et al.* (2019) The mechanisms of boronate ester formation and fluorescent turn-on in *ortho*-aminomethylphenylboronic acids. Nat. Chem. **11**, 768–778.
12) Williams, G.T., Kedge, J.L. and Fossey, J.S. (2021) Molecular boronic acid-based saccharide sensors. ACS Sens. **6**, 1508–1528.
13) Francesconi, O. and Roelens, S. (2019) Biomimetic carbohydrate-binding agents (CBAs): Binding affinities and biological activities. ChemBioChem **20**, 1329–1346.
14) Davis, A.P. (2020) Biomimetic carbohydrate recognition. Chem. Soc. Rev. **49**, 2531–2545.
15) Oki, T., Konishi, M., Tomatsu, K., Tomita, K., Saitoh, K., Tsunakawa, M. *et al.* (1988) Pradimicin, a novel class of potent antifungal antibiotics. J. Antibiot. **41**, 1701–1704.
16) Takeuchi, T., Hara, T., Naganawa, H., Okada, M., Hamada, M., Umezawa, H. *et al.* (1988) New antifungal antibiotics, benanomicins A and B from an actinomycete. J. Antibiot. **41**, 807–811.
17) Fukagawa, Y., Ueki, T., Numata, K. and Oki, T. (1993) Pradimicins and benanomicins, sugar-recognizing antibiotics: Their novel mode of antifungal action and conceptual significance. Actinomycetologica **7**, 1–22.
18) Sawada, Y., Numata, K., Murakami, T., Tanimichi, H., Yamamoto, S. and Oki, T. (1990) Calcium-dependent anticandidal action of pradimicin A. J. Antibiot. **43**, 715–721.
19) Balzarini, J., François, K.O., Van Laethem, K., Hoorelbeke, B., Renders, M., Auwerx, J. *et al.* (2010) Pradimicin S, a highly soluble nonpeptidic small-size carbohydrate-binding antibiotic, is an anti-HIV drug lead for both microbicidal and systemic use. Antimicrob. Agents Chemother. **2010**, 1425–1435.
20) Balzarini, J., Van Laethem, K., Daelemans, D., Hatse, S., Bugatti, A., Rusnati, M. *et al.* (2007) Pradimicin A, a carbohydrate-binding nonpeptidic lead compound for treatment of infections with viruses with highly glycosylated envelopes, such as human immunodeficiency virus. J. Virol. **81**, 362–373.
21) Sawada, Y., Tsuno, T., Yamamoto, H., Nishio, M., Konishi, M. and Oki, T. (1990) Pradimicins M, N, O and P, new dihydrobenzo[*a*]naphthacenequinones produced by blocked mutants of *Actino-*

madura hibisca P157-2. J. Antibiot. **43**, 1367–1374.
22) Furumai, T., Yamamoto, H., Narita, Y., Hasegawa, T., Aburaki, S., Kakushima, M. *et al.* (1993) Microbial modification of pradimicins at C-11 leading to 11-*O*-demethyl- and 11-*O*-L-xylosylpradimicins A and FA-1. J. Antibiot. **46**, 1589–1597.
23) Saitoh, K., Tsuno, T., Kakushima, M., Hatori, M., Furumai, T. and Oki, T. (1993) Pradimicin S, a new pradimicin analog II. Isolation and structure elucidation. J. Antibiot. **46**, 406–411.
24) Bauermeister, A., Calil, F.A., Pinto, F.C.L., Medeiros, T.C.T., Almeida, L.C. and Silva, L.J. (2019) Pradimicin-IRD from *Amycolatopsis* sp. IRD-009 and its antimicrobial and cytotoxic activities. J. Antibiot. **33**, 1713–1720.
25) Sawada, Y., Murakami, T., Ueki, T., Fukagawa, Y., Oki, T. and Nozawa, Y. (1991) Mannan-mediated anticandidal activity of BMY-28864, a new water-soluble pradimicin derivative. J. Antibiot. **44**, 119–121.
26) Watanabe, M., Gomi, S., Tohyama, H., Ohtsuka, K., Shibahara, S., Inouye, S. *et al.* (1996) Binding of benanomicin A to fungal cells in reference to its fungicidal action. J. Antibiot. **49**, 366–373.
27) Ueki, T., Numata, K., Sawada, Y., Nakajima, T., Fukagawa, Y. and Oki, T. (1993) Studies on the mode of antifungal action of pradimicin antibiotics I. Lectin-mimic binding of BMY-28864 to yeast mannan in the presence of calcium. J. Antibiot. **46**, 149–161.
28) Ueki, T., Numata, K., Sawada, Y., Nishio, M., Ohkura, H., Kamachi, H. *et al.* (1993) Studies on the mode of antifungal action of pradimicin antibiotics II. D-Mannopyranoside-binding site and calcium-binding site. J. Antibiot. **46**, 455–464.
29) Ueki, T., Oka, M., Fukagawa, Y. and Oki, T. (1993) Studies on the mode of antifungal action of pradimicin antibiotics III. Spectrophotometric sequence analysis of the ternary complex formation of BMY-28864 with D-mannopyranoside and calcium. J. Antibiot. **46**, 465–477.
30) Fujikawa, K., Tsukamoto, Y., Oki, T. and Lee, Y.C. (1998) Spectroscopic studies on the interaction of pradimicin BMY-28864 with mannose derivatives. Glycobiology **8**, 407–414.
31) Tamiya, M., Ohmori, K., Kitamura, M., Kato, H., Arai, T., Oorui, M. *et al.* (2007) General synthesis route to benanomicin-pradimicin antibiotics. Chemistry **13**, 9791–9823.
32) Kamachi, H., Iimura, S., Okuyama, S., Hoshi, H., Tamura, S., Shinoda, M. *et al.* (1992) Synthesis and antifungal activities of pradimicin derivatives, modification at C4′-position. J. Antibiot. **45**, 1518–1525.
33) Enomoto, M., Igarashi, Y., Sasaki, M. and Shimizu, H. (2015) A mannose-recognizable chemosensor using gold nanoparticles functionalized with pradimicin, a nonpeptidic mannose-binding natural product. Tetrahedron **71**, 2603–2609.
34) Nakagawa, Y., Masuda, Y., Yamada, K., Doi, T., Takegoshi, K., Igarashi, Y. *et al.* (2011) Solid-state NMR spectroscopic analysis of the Ca^{2+}-dependent mannose binding of pradimicin A. Angew. Chem. Int. Ed. **50**, 6084–6088.
35) Nakagawa, Y., Doi, T., Masuda, Y., Takegoshi, K., Igarashi, Y. and Ito, Y. (2011) Mapping of the primary mannose binding site of pradimicin A. J. Am. Chem. Soc. **133**, 17485–17493.
36) Nakagawa, Y. and Ito, Y. (2017). Solid-state NMR analysis of mannose recognition by pradimicin A. *In* NMR in Glycoscience and Glycotechnology (eds. Kato, K. and Peters, T.). The Royal Society of Chemistry, Cambridge, pp. 269–289.
37) Takegoshi, K., Nakamura, S. and Terao, T. (2001) ^{13}C–^{1}H dipolar-assisted rotational resonance in magic-angle spinning NMR. Chem. Phys. Lett. **344**, 631–637.
38) Takegoshi, K., Nakamura, S. and Terao, T. (2003) ^{13}C–^{1}H dipolar-driven ^{13}C–^{13}C recoupling without ^{13}C rf irradiation in nuclear magnetic resonance of rotating solids. J. Chem. Phys. **118**, 2325–2341.
39) Morcombe, C.R., Gaponenko, V., Byrd, R.A. and Zilm, K.W. (2004) Diluting abundant spins by isotope edited radio frequency field assisted diffusion. J. Am. Chem. Soc. **126**, 7196–7197.
40) Kakushima, M., Sawada, Y., Nishio, M., Tsuno, T. and Oki, T. (1989) Biosynthesis of pradimicin A. J. Org. Chem. **54**, 2536–2539.
41) Kakinuma, S., Furumai, T. and Oki, T. (1994) Biosynthesis of the pradimicin and benanomicin family of antibiotics by *Actinomadura*. Actinomycetologica **8**, 134–138.
42) Nakagawa, Y., Doi, T., Taketani, T., Takegoshi, K., Igarashi, Y. and Ito, Y. (2013) Mannose-binding geometry of pradimicin A. Chemistry **19**, 10516–10525.
43) Doi, T., Nakagawa, Y. and Takegoshi, K. (2017) Solid-state nuclear magnetic resonance analysis reveals a possible calcium binding site of pradimicin A. Biochemistry **56**, 468–472.
44) Nakagawa, Y., Doi, T., Takegoshi, K., Sugahara, T., Akase, D., Aida, M. *et al.* (2019) Molecular basis of mannose recognition by pradimicins and their application to microbial cell surface imaging. Cell Chem. Biol. **26**, 950–959.
45) Oki, T., Kakushima, M., Nishio, M., Kamei, H., Hirano, M., Sawada, Y. *et al.* (1990) Water-soluble pradimicin derivatives, synthesis and antifungal evaluation of *N*,*N*-dimethyl pradimicins. J. Antibiot. **43**, 1230–1235.
46) Watanabe, Y., Yamaji, F., Ojika, M., Sugawara, T., Akase, D., Aida, M. *et al.* (2020) The endocyclic oxygen atom of D-mannopyranose is involved in its binding to pradimicins. Tetrahedron Lett. **61**, 151530.
47) Shahzad-ul-Hussan, S., Ghirlando, R., Dogo-Isonagie, C.I., Igarashi, Y., Balzarini, J. and Bewley, C.A. (2012) Characterization and carbohydrate specificity of pradimicin S. J. Am. Chem. Soc. **134**, 12346–12349.
48) Nakagawa, Y., Yamaji, F., Miyanishi, W., Ojika, M., Igarashi, Y. and Ito, Y. (2021) Binding evaluation of pradimicins for oligomannose motifs from fungal

mannans. Bull. Chem. Soc. Jpn. **94**, 732–754.
49) Shibata, N., Ikuta, K., Imai, T., Satoh, Y., Satoh, R., Suzuki, A. *et al.* (1995) Existence of branched side chains in the cell wall mannan of pathogenic yeast, *Candida albicans*. J. Biol. Chem. **270**, 1113–1122.
50) Konradsson, P., Udodong, U.E. and Fraser-Reid, B. (1990) Iodonium promoted reactions of disarmed thioglycosides. Tetrahedron Lett. **31**, 4313–4316.
51) Suzuki, K., Maeta, H., Matsumoto, T. and Tsuchihashi, G. (1988) New glycosidation reaction 2. Preparation of 1-fluoro-D-desosamine derivative and its efficient glycosidation by the use of Cp_2HfCl_2-$AgClO_4$ as the activator. Tetrahedron Lett. **29**, 3571–3574.
52) Hanessian, S. and Banoub, J. (1977) Chemistry of the glycosidic linkage. An efficient synthesis of 1,2-*trans*-di-saccharides. Carbohydr. Res. **53**, C13–C16.
53) Nishio, M., Ohkuma, H., Kakushima, M., Ohta, S., Iimura, S., Hirano, M. *et al.* (1993) Synthesis and antifungal activities of pradimicin A derivatives. Modification of the alanine moiety. J. Antibiot. **46**, 494–499.
54) Nakagawa, Y., Kakihara, S., Tsuzuki, K., Ojika, M., Igarashi, Y. and Ito, Y. (2021) A pradimicin-based staining dye for glycoprotein detection. J. Nat. Prod. **84**, 2496–2501.
55) Saba, J.A., Shen, X., Jamieson, J.C. and Perreault, H. (2001) Investigation of different combinations of derivatization, separation methods and electrospray ionization mass spectrometry for standard oligosaccharides and glycans from ovalbumin. J. Mass Spectrom. **36**, 563–574.
56) Szabo, Z., Thayer, J.R., Agroskin, Y., Lin, S., Liu, Y., Srinivasan, K. *et al.* (2017) In-depth analyses of native N-linked glycans facilitated by high-performance anion exchange chromatography-pulsed amperometric detection coupled to mass spectrometry. Anal. Bioanal. Chem. **409**, 3089–3101.
57) Hu, Y., Shihab, T., Zhou, S., Wooding, K. and Mechref, Y. (2016) LC-MS/MS of permethylated N-glycans derived from model and human blood serum glycoproteins. Electrophoresis **37**, 1498–1505.
58) Satomi, Y., Shimonishi, Y., Hase, T. and Takao, T. (2004) Site-specific carbohydrate profiling of human transferrin by nano-flow liquid chromatography/electrospray ionization mass spectrometry. Rapid Commun. Mass Spectrom. **18**, 2983–2988.
59) Flynn, G.C., Chen, X., Liu, Y.D., Shah, B. and Zhang, Z. (2010) Naturally occurring glycan forms of human immunoglobulins G1 and G2. Mol. Immunol. **47**, 2074–2082.

(Received Sep. 21, 2021; accepted Nov. 11, 2021)

Profile

Yu Nakagawa was born in Shiga Prefecture, Japan, in 1974. He graduated from Kyoto University in 1997 and obtained his Ph.D. degree in Agriculture from the same university in 2002. He was a research fellow of the Japan Society for the Promotion of Science (DC1, PD) under direction of Prof. Kazuhiro Irie at Kyoto University from 1999 to 2005. He joined the laboratory of Professor Paul A. Wender at Stanford University as a postdoctoral fellow from 2005 to 2006. After an additional 2 years of postdoctoral training in Professor Irie's group at Kyoto University, he joined Dr. Yukishige Ito's group at RIKEN in 2008 as a research scientist, and was promoted to a senior research scientist in 2010. Since 2014, he has been an associate professor at Nagoya University. He received the Young Scientist's Research Award in Natural Product Chemistry (2009) and Japan Society for Bioscience, Biotechnology, and Agrochemistry Award for the Encouragement of Young Scientists (2011). His current research interests include the discovery of functionally unique natural products and their application for biological research.

Profile

Yukishige Ito was born in Hyogo Prefecture in 1954 and graduated from The University of Tokyo in 1977. After receiving his Ph.D. degree in Pharmaceutical Sciences in 1982 (supervisor, Professor Masaji Ohno), he carried out postdoctoral work in the U.S.A. at Massachusetts Institute of Technology (advisor, Professor Satoru Masamune). In 1984, he returned to Japan as a Research Scientist at RIKEN and started his career in carbohydrate chemistry under the supervision of Dr. Tomoya Ogawa. In 1998, he became an independent researcher in the same institute and directed his research group as a Chief Scientist until 2020. From 2009 to 2015, he was jointly appointed as a Research Director of a JST ERATO project. Currently, he is affiliated with the Graduate School of Science, Osaka University as a Specially Appointed Professor. The major focus of his research has been directed to the development of methodologies for the chemical synthesis of complex oligosaccharides and glycoconjugates and analysis of the biological functions of glycoproteins and glycolipids. In recognition of his contribution to carbohydrate chemistry and chemical glycobiology, he has received domestic and international awards including the Roy L. Whistler International Award in Carbohydrate Chemistry (2008), Takeda Award for International Achievements (2010), Japan Society for Bioscience, Biotechnology, and Agrochemistry Award (2012), Synthetic Organic Chemistry Award, Japan (2017), and ACS Claude S. Hudson Award (2021).